



THE UNIVERSITY *of* EDINBURGH

Edinburgh Research Explorer

Metal-Insulator Transition and Orbital Order in PbRuO₃

Citation for published version:

Kimber, SAJ, Rodgers, JA, Wu, H, Murray, CA, Argyriou, DN, Fitch, AN, Khomskii, DI & Attfield, JP 2009, 'Metal-Insulator Transition and Orbital Order in PbRuO₃', *Physical Review Letters*, vol. 102, no. 4, 046409, pp. -. <https://doi.org/10.1103/PhysRevLett.102.046409>

Digital Object Identifier (DOI):

[10.1103/PhysRevLett.102.046409](https://doi.org/10.1103/PhysRevLett.102.046409)

Link:

[Link to publication record in Edinburgh Research Explorer](#)

Document Version:

Publisher's PDF, also known as Version of record

Published In:

Physical Review Letters

Publisher Rights Statement:

Copyright © 2009 by the American Physical Society. This article may be downloaded for personal use only. Any other use requires prior permission of the author(s) and the American Physical Society.

General rights

Copyright for the publications made accessible via the Edinburgh Research Explorer is retained by the author(s) and / or other copyright owners and it is a condition of accessing these publications that users recognise and abide by the legal requirements associated with these rights.

Take down policy

The University of Edinburgh has made every reasonable effort to ensure that Edinburgh Research Explorer content complies with UK legislation. If you believe that the public display of this file breaches copyright please contact openaccess@ed.ac.uk providing details, and we will remove access to the work immediately and investigate your claim.



Metal-Insulator Transition and Orbital Order in PbRuO_3

Simon A. J. Kimber,^{1,2} Jennifer A. Rodgers,² Hua Wu,³ Claire A. Murray,² Dimitri N. Argyriou,¹ Andrew N. Fitch,⁴
Daniel I. Khomskii,^{3,5} and J. Paul Attfield^{2,*}

¹*Helmholtz-Zentrum Berlin für Materialien und Energie, 100 Glienicker Straße, 14109 Berlin, Germany*

²*Centre for Science at Extreme Conditions and School of Chemistry, University of Edinburgh, King's Buildings,
Mayfield Road, Edinburgh EH9 3JZ, United Kingdom*

³*II. Physikalisches Institut, Universität zu Köln, Zùlpicher Straße 77, D-50937 Köln, Germany*

⁴*European Synchrotron Radiation Facility, B.P. 220, 38043 Grenoble Cedex, France*

⁵*Department of Physics, Loughborough University, Leicestershire LE11 3TU, United Kingdom*

(Received 20 November 2008; published 29 January 2009)

Anomalous low temperature electronic and structural behavior has been discovered in PbRuO_3 . The structure [space group $Pnma$, $a = 5.563\,14(1)$, $b = 7.864\,68(1)$, $c = 5.614\,30(1)$ Å] and metallic conductivity at 290 K are similar to those of SrRuO_3 and other ruthenate perovskites, but a sharp metal-insulator transition at which the resistivity increases by 4 orders of magnitude is discovered at 90 K. This is accompanied by a first-order structural transition to an $Imma$ phase [$a = 5.569\,62(1)$, $b = 7.745\,50(1)$, $c = 5.662\,08(1)$ Å at 25 K] that shows a coupling of Ru^{4+} 4d orbital order to distortions from Pb^{2+} 6s6p orbital hybridization. The $Pnma$ to $Imma$ transition is an unconventional reversal of the group-subgroup symmetry relationship. No long range magnetic order is evident down to 1.5 K. Calculations show that Pb 6s6p and Ru 4d orbital hybridization and strong spin-orbit coupling are significant.

DOI: 10.1103/PhysRevLett.102.046409

PACS numbers: 71.30.+h, 61.66.Fn, 71.20.Ps

Transition metal oxide perovskites display a remarkable range of electronic phenomena such as superconductivity, colossal magnetoresistances, and coupled charge, orbital, and spin orderings [1]. Perovskite-related ruthenates based on Ru^{4+} have proved interesting as broad Ru : 4d bands lead to metallicity without chemical doping, so very clean correlated itinerant electron physics may be observed in single crystals. The layered perovskite Sr_2RuO_4 is a p -wave superconductor [2], while bilayered $\text{Sr}_3\text{Ru}_2\text{O}_7$ is a metallic metamagnet [3]. All of the cubic-type ARuO_3 perovskites ($A = \text{Ca}, \text{Sr}, \text{Ba}$) are metallic to the lowest measured temperatures. SrRuO_3 and BaRuO_3 are ferromagnets with Curie temperatures of $T_C = 160$ and 60 K, respectively [4–7], but CaRuO_3 does not show a magnetic transition [8]. Another ruthenate perovskite, PbRuO_3 , was synthesized at high pressures in 1970 [9], but the electronic properties of this material have not been reported. Pb^{2+} is intermediate in size between Sr^{2+} and Ba^{2+} , so PbRuO_3 is expected to be a ferromagnetic metal. However, in this Letter, we report that PbRuO_3 behaves very differently from the other ARuO_3 perovskites and instead shows a sharp metal-insulator transition at 90 K but without apparent long range spin order. Electron localization is strongly coupled to the lattice through Ru-orbital ordering, resulting in an anomalous structural change to higher lattice symmetry at low temperatures. We propose that strong hybridization of Ru 4d with Pb 6s and 6p states and spin-orbit coupling are responsible for inducing this alternative ground state for ruthenate perovskites.

Small (ca. 10 mg) polycrystalline pellets of PbRuO_3 were synthesized by heating the oxygen-deficient pyrochlore $\text{Pb}_2\text{Ru}_2\text{O}_{6.5}$ at 11 GPa and 1100 °C using a

Walker-type multianvil press. Synchrotron x-ray diffraction profiles in the temperature range $10 < T < 300$ K were collected from instrument ID31 at the ESRF, France, with wavelength $\lambda = 0.45\,621$ Å, and time-of-flight neutron powder data were recorded using the GEM spectrometer at ISIS, United Kingdom, over the range $1.5 < T < 300$ K. Rietveld fits to diffraction data were performed using the GSAS package [10]. Magnetic susceptibility and electronic resistivity measurements were made using Quantum Design MPMS and PPMS (Magnetic and Physical Properties Measurement System) instruments.

The (hkl) Bragg reflections observed in the room temperature x-ray and neutron powder diffraction profiles of PbRuO_3 are all consistent with the orthorhombic $Pnma$ space group of SrRuO_3 [11], and refinement of this model gave good fits to the data. We also attempted refinements of noncentrosymmetric variants of this structure, in case of a steric (“lone pair”) effect from the Pb 6s² state, but no improvements were obtained and the fits diverged. All of the site occupancies refined to within error (ca. 1%) of full occupancy, showing that the sample is stoichiometric [12]. The $Pnma$ superstructure is often observed in oxide perovskites and results from a generic, oxygen-centered, tilting instability rather than specific, transition metal-centered electronic instabilities.

To compare the contributions of Pb^{2+} and Sr^{2+} to the ruthenate band structures, we performed electronic structure calculations for room temperature $Pnma$ -type PbRuO_3 and SrRuO_3 [13] in the local density approximation (LDA) using the full-potential augmented plane wave plus local orbital method [14]. The results (Fig. 1) for SrRuO_3 are very similar to those previously reported [5].

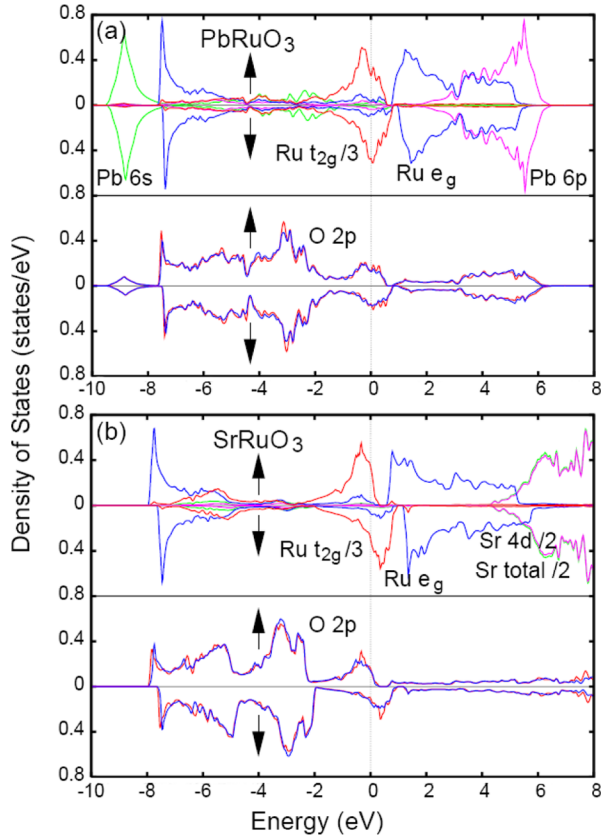


FIG. 1 (color online). Density of states (DOS) of (a) PbRuO_3 and (b) SrRuO_3 in the $Pnma$ structure calculated by the LDA in the ferromagnetic state. Up (down) arrows refers to spin up (down). The $\text{Ru } t_{2g}$ DOS is scaled by $\frac{1}{3}$, and the Sr DOS is scaled by $\frac{1}{2}$. The exchange splitting of the $\text{Ru } t_{2g}$ - $\text{O } 2p$ bands is significantly suppressed in PbRuO_3 .

The Sr^{2+} states lie far from the $\text{Ru } 4d$ - $\text{O } 2p$ bands near the Fermi level [6], and a large exchange splitting is found. The itinerant ferromagnetic state is stabilized by 25 meV/f.u., in keeping with the 160 K Curie transition. By contrast, the $\text{Ru } 4d$ and $\text{O } 2p$ states in PbRuO_3 lie just between the occupied $\text{Pb } 6s$ and unoccupied $\text{Pb } 6p$ states. The $\text{Ru } t_{2g}$ - $\text{Pb } 6s$ and $\text{Ru } e_g$ - $\text{Pb } 6p$ hybridizations, both aided by the $\text{O } 2p$ state, and t_{2g} - e_g mixing due to the lattice distortion, significantly suppress the exchange splitting of the $\text{Ru } t_{2g}$ - $\text{O } 2p$ conduction bands, reducing the magnetic stabilization energy to near zero (<4 meV/f.u.). To confirm that the slight lattice differences between the two materials are unimportant, we also calculated the electronic structure of SrRuO_3 using the PbRuO_3 parameters and found that the electronic and magnetic properties were virtually identical.

An unexpected difference between PbRuO_3 and the other perovskite ruthenates was discovered by resistivity measurements (Fig. 2). At ambient temperatures, the PbRuO_3 has a resistivity of $\sim 10^{-1} \Omega \text{ cm}$ with little temperature dependence, characteristic of metallic conduction with a resistive grain boundary contribution. However, on cooling, the resistivity increases sharply by 4 orders of

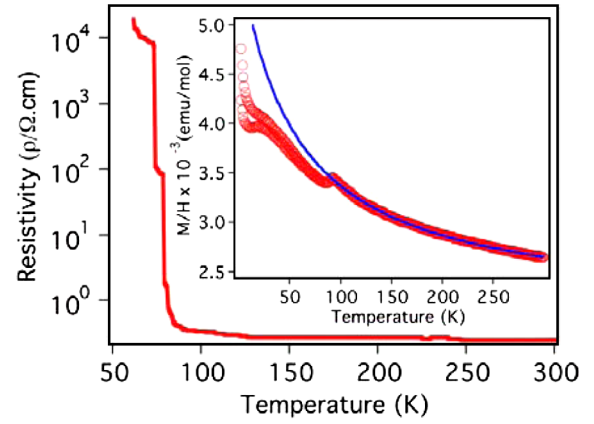


FIG. 2 (color online). Resistivity variation for PbRuO_3 ; the inset shows magnetic susceptibility measured in a 1 T field with a modified Curie-Weiss fit as described in the text.

magnitude (and was immeasurably large below 60 K), signifying a metal-insulator transition at $T_{\text{MI}} = 90$ K. This transition is also evident in magnetization data. The high temperature susceptibility is fitted as $\chi = C/(T - \theta) + \chi_p$, a sum of Curie-Weiss and Pauli paramagnetic terms, respectively, with $\chi_p = 2.09(1) \times 10^{-3} \text{ emu/mol}$, Curie constant $C = 0.195 \text{ emu K/mol}$ (corresponding to a paramagnetic moment of $1.25 \mu_B$), and a Weiss temperature $\theta = -54$ K. Similar large temperature-independent contributions have been reported for nonperovskite ruthenates such as the pyrochlore $\text{Ti}_2\text{Ru}_2\text{O}_7$ ($\chi_p \approx 2 \times 10^{-3} \text{ emu/mol}$) [15] close to metal-insulator instabilities. A small dip is observed in the magnetic susceptibility on cooling through T_{MI} , showing that antiferromagnetic correlations are present in the insulating state. However, no long range magnetic transition is evident down to 4 K, although a broad hump with divergence between field- and zero-field-cooled susceptibilities is observed below 50 K.

A strong coupling of structure to the metal-insulator transition is observed in both x-ray and neutron powder diffraction measurements (Fig. 3). PbRuO_3 remains orthorhombic down to 1.5 K; however, the lattice parameters and volume change discontinuously on cooling through the transition (Fig. 4), and, surprisingly, the $Pnma$ superstructure reflections with odd $(h + k + l)$ values disappear (see Fig. 3 inset). No new superstructure reflections, peak broadenings, or splittings were observed in the low temperature diffraction patterns of PbRuO_3 , which are indexed by the body-centered space group $Imma$. This describes another common tilting superstructure of perovskites, and a refined $Imma$ model gives excellent fits to both x-ray and neutron data [12]. Fits of lower-symmetry, acentric body-centered structures were unsuccessful. No magnetic diffraction peaks were observed down to 1.5 K in the GEM time-of-flight neutron diffraction data or in subsequent constant wavelength profiles collected from instrument E6 at the HZB reactor. We estimate the upper limit for any ordered Ru moment to be $\sim 0.5 \mu_B$.

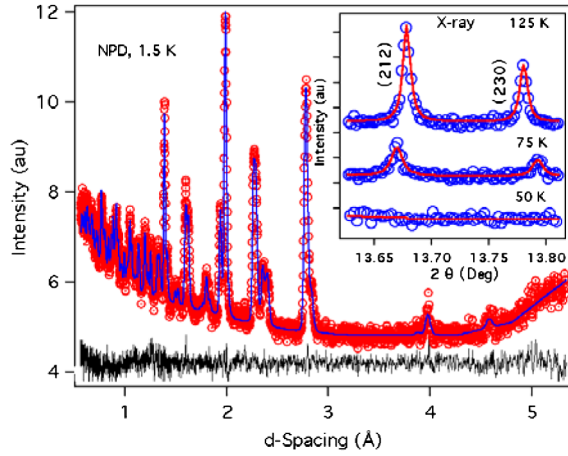


FIG. 3 (color online). Fit of the *Imma* model to the time-of-flight neutron diffraction profile of PbRuO_3 at 1.5 K. The inset shows the disappearance of *Pnma* x-ray superstructure reflections as the *Imma* phase is formed on cooling.

The (high temperature) *Pnma* to (low temperature) *Imma* transition in PbRuO_3 is remarkable as *Pnma* is a subgroup of *Imma*, so a continuous group-subgroup transition from *Imma* to *Pnma* is allowed in Landau theory and is observed in many simple perovskites such as SrSnO_3 [16]. The *Pnma-Imma* “subgroup-group” transition in PbRuO_3 is clearly first-order, with a small volume anomaly typical of metal-insulator transitions and a substantial hysteresis of 20 K in the cell parameters between warming and cooling experiments (Fig. 4). The subgroup-group structural contribution to the transition entropy is negative, but this is evidently outweighed by the large positive electronic contribution from the delocalization of Ru 4d electrons.

The evolution of the Ru-O bond distances (Fig. 4) reveals an important aspect of the metal-insulator transition. At room temperature, the RuO_6 octahedra are almost regular with Ru-O bond lengths of 2.00–2.01 Å, but, below T_{MI} , a Jahn-Teller distortion is apparent in the *Imma* structure, with two short Ru-O1 bonds (1.97 Å) aligned approximately along *z* and four long Ru-O2 bonds (2.02 Å) in the *xy* plane. To a first approximation, this corresponds to a $d_{xy}^2 d_{xz}^1 d_{yz}^1$ orbital ordering of the $\text{Ru}^{4+} t_{2g}^4$ configuration in the insulating *Imma* phase, creating planes of minority-spin-occupied d_{xy} orbitals, as shown in Fig. 4. Pb^{2+} shows an unusual A-site distortion, having a near-regular square pyramidal coordination with five short Pb-O bonds (Pb-O1, 2.51 Å \times 1; Pb-O2, 2.50 Å \times 4), while other Pb-O distances are >2.82 Å. The O1-Ru-O2 angle of 122.5° shows that this is not a lone pair effect, for which an angle of $<90^\circ$ is expected. The Pb and Ru distortions are cooperative as O1 forms short bonds to Ru and only one short bond to Pb, whereas O2 has long bonds to Ru and four short bonds to Pb.

To clarify the orbitally ordered state, we have carried out LSDA + *U* calculations for the *Imma* phase with an effective Hubbard $U = 3.5$ eV [17]. Spin-orbit coupling (SOC) was also included since this ~ 160 meV interaction

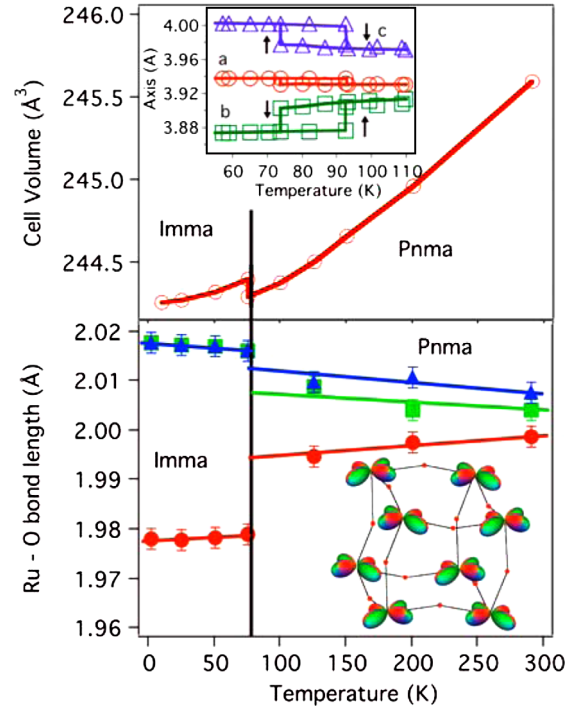


FIG. 4 (color online). Cell volume (top) and Ru-O distance (bottom) variations for PbRuO_3 from fits to neutron diffraction data. The upper inset shows hysteresis in the lattice parameters, normalized to the cubic perovskite cell, from x-ray measurements while warming or cooling at 10 K/min. Idealized d_{xy} orbital order in the *Imma* phase is shown in the lower panel.

is large relative to the calculated crystal field splitting between the d_{xy} and d_{xz}/d_{yz} levels of ~ 50 meV. Our LSDA + *U* + SOC calculations gave an insulating ground state with a small gap of ~ 0.1 eV, verifying that PbRuO_3 is in the vicinity of a metal-insulator transition. The minority spin electron has a $0.46(1+i)d_{xy} - 0.38(1-i)(d_{xz} + d_{yz})$ orbital state which consists of 42% d_{xy} , 29% d_{xz} , and 29% d_{yz} , with d_{xy} being dominant as expected from the above structural results. Different magnetic solutions lie close in energy; e.g., the lowest *G*-type antiferromagnetic state is only 6.8 meV/f.u. below the ferromagnetic state, in keeping with the observed lack of magnetic order discussed below.

The insulating, orbitally ordered ground state of PbRuO_3 is anomalous in comparison to the other ARuO_3 perovskites ($A = \text{Ca, Sr, Ba}$), which remain metallic to the lowest temperature. This is not due to a size effect as CaRuO_3 has the most tilted *Pnma* superstructure but is stable to orbital order. (The combination of small Ca^{2+} and an imposed tetragonal symmetry in layered Ca_2RuO_4 is sufficient to induce a weak orbital order [18], but this phase is a Mott insulator.) The electronic nature of Pb is a key factor, and Ru 4d-Pb 6s6p-O 2p hybridizations are evident in the above band structure calculations. This Pb^{2+} covalency is sometimes manifest as a lone pair distortion resulting in ferroelectricity, e.g., in PbTiO_3 , but lone pair distortions are not observed in either the *Pnma* or the

Imma phases of PbRuO_3 . Another consequence of covalency is the stabilization of lower Pb^{2+} coordination numbers than expected from cation size arguments [19] as shown by the change from three short (2.47 Å) Pb-O bonds in the *Pnma* structure of PbRuO_3 to five, described above, in the *Imma* phase. The metal-insulator transition in PbRuO_3 is thus driven by electronic instabilities of both cations as the orbital order of $t_{2g}^4\text{Ru}^{4+}$ is coupled to an order of $s^2p^0\text{Pb}^{2+}$ hybrid states. By contrast, Ru-orbital order is suppressed, and the metallic state remains stable in the other ARuO_3 perovskites that lack A-cation instabilities.

Orbital order lowers magnetic dimensionality relative to the structural dimensionality, and this can open a spin gap in some nonperovskite ruthenates, e.g., a singlet dimerized phase in $\text{La}_4\text{Ru}_2\text{O}_{10}$ [20,21] and possible Haldane chains in $\text{Ti}_2\text{Ru}_2\text{O}_7$ [15]. This seems not to be the case here; however, the observation of a broad susceptibility maximum at 25 K and the lack of a long range magnetic transition down to 1.5 K, which in conjunction with a Weiss temperature of -54 K corresponds to a frustration factor $|\theta/T_c| > 36$, shows that PbRuO_3 does not have a conventional ordered magnetic ground state. The divergence of field- and zero-field-cooled susceptibilities evidences some glassy character to the ground state, but there is no obvious source for structural disorder. One possibility is that the combination of orbital order and octahedral tilting (which gives a Ru-O-Ru angle of 159.8°) weakens nearest neighbor antiferromagnetic superexchange interactions in the *xy* plane so that they become comparable to the next nearest neighbor couplings. This frustrates spin order in the *xy* plane, leading to one-dimensional (*z* direction) magnetic behavior in the three-dimensional perovskite lattice imposed by orbital order.

In summary, the low temperature properties of PbRuO_3 show that normally hidden orbitally ordered states such as that of degenerate $t_{2g}^4\text{Ru}^{4+}$ ions in ruthenate perovskites may be stabilized by coupling to electronic instabilities of other cations. This may provide a strategy for accessing orbitally ordered states of other *4d* and *5d* transition metal oxide networks. The combined order of Pb *s* and *p* hybridized orbitals, Ru *d* orbitals, and O-centered octahedral tilting instabilities results in an anomalously high symmetry ground state structure that inverts the usual group-subgroup symmetry descent. These distortions also suppress long range spin order in PbRuO_3 , and further experiments and theoretical work will be needed to elucidate the magnetic ground state.

We acknowledge EPSRC for support and the provision of ESRF and ISIS beam time and the Leverhulme trust for additional support. H.W. and D.I.K. are supported by DFG through SFB 608. We thank J.W.G. Bos (Edinburgh), P.G. Radaelli (ISIS), and N. Stüer, A. Buchsteiner, and D.A. Tennant (HZB) for assistance with diffraction measurements and useful discussions.

*Corresponding author.

j.p.attfield@ed.ac.uk

- [1] Y. Tokura, Rep. Prog. Phys. **69**, 797 (2006).
- [2] K. Ishida *et al.*, Nature (London) **396**, 658 (1998).
- [3] S. A. Grigera *et al.*, Science **294**, 329 (2001).
- [4] J. M. Longo, P. M. Raccach, and J. B. Goodenough, J. Appl. Phys. **39**, 1327 (1968).
- [5] D. J. Singh, J. Appl. Phys. **79**, 4818 (1996).
- [6] I. I. Mazin and D. J. Singh, Phys. Rev. B **56**, 2556 (1997).
- [7] C.-Q. Jin *et al.*, Proc. Natl. Acad. Sci. U.S.A. **105**, 7115 (2008).
- [8] L. Klein *et al.*, Phys. Rev. B **60**, 1448 (1999).
- [9] J. A. Kafalas and J. M. Longo, Mater. Res. Bull. **5**, 193 (1970).
- [10] A. C. Larson and R. B. Von Dreele, Report No. LAUR 86-748, 1998.
- [11] C. W. Jones, P. D. Battle, P. Lightfoot, and W. T. A. Harrison, Acta Crystallogr. Sect. C **45**, 365 (1989).
- [12] Refined *x*, *y*, and *z* coordinates and isotropic *U* factors for neutron refinements of PbRuO_3 in space group *Pnma* at 290 K [and in *Imma* at 25 K where different]: Pb: 0.0120 (5) [0], 0.25, 0.9955(4) [0.9868(1)], and 0.0075(3) Å² [0.0001(1) Å²]; Ru: 0, 0, 0.5, and 0.0026(3) Å² [0.0010(1) Å²]; O1: 0.4991(1) [0.5], 0.25, 0.0638(5) [0.0705(2)], and 0.0077(5) Å² [0.0032(2) Å²]; O2: 0.2745(4) [0.25], 0.0359(2) [0.0456(1)], 0.7255(4) [0.75], and 0.0088(4) Å² [0.0034(1) Å²]. Cell parameters are shown in the abstract. Reduced chi-squared = 1.27 [1.77] and weighted profile residual $R_{wp} = 0.022$ [0.026].
- [13] H. Kobayashi, M. Nagata, R. Kanno, and Y. Kawamoto, Mater. Res. Bull. **29**, 1271 (1994).
- [14] P. Blaha, K. Schwarz, G. K. H. Madsen, D. Kvasnicka, and J. Luitz, WIEN2K code, <http://www.wien2k.at>. The muffin-tin sphere radii were 2.5, 2.1, and 1.5 Bohr for Pb(Sr), Ru, and O, respectively, the cutoff energy of the plane wave expansion was set at 16 Ryd, and 1600 *k* points were used for integration over the Brillouin zone. Structural relaxations gave lattice constants only 1.2% smaller than the experimental ones and atomic displacements ≤ 0.02 Å.
- [15] S. Lee *et al.*, Nature Mater. **5**, 471 (2006).
- [16] E. H. Mountstevens, S. A. T. Redfern, and J. P. Attfield, Phys. Rev. B **71**, 220102(R) (2005).
- [17] *U* was calculated following G. K. H. Madsen and P. Novák, Europhys. Lett. **69**, 777 (2005).
- [18] I. Zegkinoglou, Phys. Rev. Lett. **95**, 136401 (2005).
- [19] Hence a high pressure is needed to increase the Pb oxygen coordination from 8 in the ideal pyrochlore structure of $\text{PbRuO}_{3(+x)}$ to 12 in the ideal perovskite arrangement, while SrRuO_3 is thermodynamically stable at ambient pressure. This effect is also evident in the room temperature *Pnma* perovskite structures. The lattice parameters of PbRuO_3 are slightly larger than those for SrRuO_3 ($a = 5.535$, $b = 7.851$, $c = 5.572$ Å), but the three short (< 2.6 Å) Pb-O distances in PbRuO_3 ($2.47 \text{ Å} \times 3$) are shorter than the corresponding Sr-O distances in SrRuO_3 (2.51×1 and 2.52×2 Å).
- [20] P. Khalifah *et al.*, Science **297**, 2237 (2002).
- [21] H. Wu *et al.*, Phys. Rev. Lett. **96**, 256402 (2006).